Development 130, 3147-3161

doi:10.1242/dev.00518

UNC-71, a disintegrin and metalloprotease (ADAM) protein, regulates motor axon guidance and sex myoblast migration in *C. elegans*

Xun Huang[1], Peng Huang[2], Matthew K. Robinson[2,*], Michael J. Stern[2] and Yishi Jin[1,3,†]

[1]Department of Molecular, Cellular and Developmental Biology, Sinsheimer Laboratories, University of California, Santa Cruz, CA 95064, USA
[2]Department of Genetics, Yale University School of Medicine, New Haven, CT 06520-8005, USA
[3]Howard Hughes Medical Institute, University of California, Santa Cruz, CA 95064, USA
*Present address: Fox Chase Cancer Center, Medical Oncology, 7701 Burholme Avenue, Philadelphia, PA 19111, USA
†Author for corrrespondence (e-mail: jin@biology.ucsc.edu)

Accepted 31 March 2003

SUMMARY

The migration of cells and growth cones is a process that is guided by extracellular cues and requires the controlled remodeling of the extracellular matrix along the migratory path. The ADAM proteins are important regulators of cellular adhesion and recognition because they can combine regulated proteolysis with modulation of cell adhesion. We report that the *C. elegans* gene *unc-71* encodes a unique ADAM with an inactive metalloprotease domain. Loss-of-function mutations in *unc-71* cause distinct defects in motor axon guidance and sex myoblast migration. Many *unc-71* mutations affect the disintegrin and the cysteine-rich domains, supporting a major function of *unc-71* in cell adhesion. UNC-71 appears to be expressed in a selected set of cells. Genetic mosaic analysis and tissue-specific expression studies indicate that *unc-71* acts in a cell non-autonomous manner for both motor axon guidance and sex myoblast migration. Finally, double mutant analysis of *unc-71* with other axon guidance signaling molecules suggests that UNC-71 probably functions in a combinatorial manner with integrins and UNC-6/netrin to provide distinct axon guidance cues at specific choice points for motoneurons.

Key words: ADAM, Axon guidance, Migration, *C. elegans*, UNC-71, ADM-1, Netrin, Integrin

INTRODUCTION

The migration of cells and growth cones requires dynamic interactions between cells and the extracellular matrix along the migratory path. The ADAM (for a disintegrin and metalloprotease) family of proteins has been implicated as important regulators of such interactions for their dual activities: proteolysis and cell adhesion (Wolfsberg et al., 1995; Primakoff and Myles, 2000; Seals and Courtneidge, 2003). This family includes a large number of transmembrane proteins that are present from *S. pombe* to human (www.gene.ucl.ac.uk/nomenclature/genefamily/metallo.html), and share a conserved multi-domain organization. All ADAM proteins have an N-terminal signal sequence followed by a prodomain, a metalloprotease domain, a disintegrin domain, a cysteine-rich region that usually contains an EGF repeat, a transmembrane domain and a cytoplasmic tail (Schlondorff and Blobel, 1999; Primakoff and Myles, 2000; Seals and Courtneidge, 2003). The functional importance of ADAM proteins is highlighted by their involvement in the regulation of the Notch pathway, sperm and egg recognition, and asthma hyper-responsiveness (Bigler et al., 1997; Lieber et al., 2002; van Eerdewegh et al., 2002). However, the physiological roles for many ADAMs have yet to be elucidated.

Most biochemical studies have focused on two functional modules of ADAM proteins: proteolysis of membrane receptors by the metalloprotease domain, and interaction with integrins by the disintegrin domain. The metalloprotease domain is composed of ~200 amino acids, and protease activity depends on a conserved zinc-binding catalytic site sequence HExGHxxGxxHD, in which the three histidines bind zinc and the glutamic acid is the catalytic residue. Proteolysis of extracellular domains of transmembrane proteins by ADAMs, a process also known as ectodomain shedding, has been shown to be important for several signaling events (Black and White, 1998). For example, the *Drosophila* Kuzbanian and its orthologs in other species (Kuz/ADAM10 family) process the Notch receptor and its ligand Delta in a conserved manner (Rooke et al., 1996; Pan and Rubin, 1997; Qi et al., 1999; Lieber et al., 2002). Kuz also modulates axon repulsion by releasing the ephrin ligand (Hattori et al., 2000), and axon extension, possibly through shedding and releasing of the netrin receptor DCC (Fambrough et al., 1996; Galko and Tessier-Lavigne, 2000). However, nearly half of the known ADAMs have amino acid substitutions within the catalytic site sequence, and are likely to be inactive metalloproteases (Black and White, 1998). It has been proposed that inactive ADAMs may regulate the activity of an ADAM with active protease

through protein complex formation (Pan and Rubin, 1997). For example, fertilin β/ADAM2, an inactive metalloprotease, forms a heterodimeric protein complex with fertilin α/ADAM1, an active ADAM, and functions in sperm-egg fusion (Waters and White, 1997; Cho et al., 2000). However, definitive evidence for this hypothesis is still lacking.

The disintegrin domain, which is named after the soluble snake venom (SVMP) disintegrin (Gould et al., 1990), is composed of about 100 amino acids, within which is a disintegrin loop containing three invariant cysteines ($CX_{5-6}CX_5C$) (Wolfsberg et al., 1995). In a canonical disintegrin domain in SVMPs, the disintegrin loop has the integrin-binding RGD tripeptide and can inhibit integrin functions in vitro. However, only one ADAM has the RGD tripeptide, and the others have divergent sequences that usually contain a conserved Arg next to the first cysteine and a conserved aspartic acid next to the second cysteine. The interaction between non-RGD containing ADAMs with integrins is not well understood. It has been shown that fertilin β, ADAM9, ADAM12, ADAM23 and ADAM28 can bind many integrins (reviewed by Evans, 2001), and that integrin α9β1 can bind all ADAMs except ADAM10 and ADAM17 (Eto et al., 2002). The functions of the cysteine-rich region and other domains of ADAMs are much less studied, although it has been suggested that the cysteine-rich domain may mediate cell fusion and adhesion, and that the prodomain may regulate the protease activity (Primakoff and Myles, 2000).

The nematode *C. elegans* has four ADAM genes (*adm-1*, *adm-2*, *adm-4* and *sup-17*), and one secreted ADAM-like gene (*mig-17*) (The *C. elegans* Genome Consortium, 1998). SUP-17 is the Kuz/ADAM10 ortholog and regulates LIN-12/Notch signaling pathway in vulva formation (Wen et al., 1997). MIG-17 is required for the distal tip cell migration during gonadogenesis (Nishiwaki et al., 2000). We report that the *unc-71* gene corresponds to *adm-1*, which has previously been identified through homology search (Podbilewicz, 1996). *unc-71* was defined by a single allele in the original general screen for *C. elegans* mutants (Brenner, 1974). Since then, a number of different screens have identified many additional alleles of *unc-71* (Chen et al., 1997; Huang et al., 2002). Previous characterizations of *unc-71* mutants have revealed important functions of *unc-71* in various aspects of axon guidance, including axon fasciculation of the ventral and dorsal nerve cords, and axonal morphogenesis of the HSNs and the phasmid neurons (Siddiqui, 1990; Siddiqui and Culotti, 1991; McIntire et al., 1992). *unc-71* also plays a role in one of the mechanisms known to help guide the migrations of the hermaphrodite sex myoblasts (Chen et al., 1997). The unification of the genetic and phenotypic characterizations of *unc-71* alleles with the molecular identity of *unc-71/adm-1* has allowed us to undertake a more detailed analysis of the role of this ADAM in these important processes.

MATERIALS AND METHODS

Strains and genetics

C. elegans were grown on NGM plates under standard conditions as described by Brenner (Brenner, 1974). For snip-SNP mapping of *unc-71*, recombinants were isolated from *dpy-18(e364) unc-71(e541)/CB4856* heterozygotes. 21/28 Dpy nonUnc recombinants segregated *SNP(III)+17.4* and 28/28 Dpy nonUnc recombinants segregated *SNP(III)+20.1*. The deletion alleles were obtained from S. Mitani (Japan) and *C. elegans* knockout consortium. The precise lesions are as follows. *adm-2(tm347)* is a 1363 bp deletion that removes the region from third intron to exon 8; and *inb-1(tm353)* is a 800 bp deletion that removes the last amino acid in exon 5 and most of the intron 5 (S. Mitani, personal communication). *adm-4(ok265)* is a 847 bp deletion with a extra C insertion. Other strains were generated by us or obtained from CGC. Double mutants were constructed following standard procedures, and were confirmed by phenotypic analysis and backcrossing. The presence of *adm-2*, *adm-4* and *inb-1* mutations in the double mutants was confirmed by PCR.

Molecular biology of *unc-71*

Cosmids and YAC clones were obtained from the Sanger Centre (Hinxton, UK). DNA manipulations were performed following standard procedures (Sambrook et al., 1989). The *unc-71/adm-1* genomic region was amplified using long range PCR kit (Roche, Indianapolis, IN). The DNA pool that rescued *unc-71* contained three overlapping PCR products that covered the entire coding region with 6.6 kb 5′ upstream and 0.7 kb 3′ downstream sequences. *unc-71* minigene (pCZ418) was generated by placing into the cDNA yk344a1 the *Eco*RV genomic fragment (–47 to +1641) containing the first intron and the *Kpn*I-*Spe*I genomic fragment (+3132 to +7149) containing the last intron, last exon and 1018 bp 3′ UTR. To generate the *unc-71* metalloprotease domain deletion clone (pCZ423), a 441 bp *Bst*Z17I-*Ssp*I fragment in pCZ418 was deleted. To generate the *unc-71* C-terminal truncation clone, a 3.3 kb *Bbs*I-*Spe*I fragment in pCZ418 was deleted. A second *unc-71* minigene (NH#1092) was constructed by cloning the *Bgl*II-*Mfe*I (–132 to +1795) genomic fragment and the *Mfe*I(+236)-*Apa*I (a site in the vector) cDNA fragment from yk344a1 clone into the *Bam*HI-*Apa*I sites of pBluescript II KS(+). The two minigenes behaved very similarly in transformation rescue assays. To generate the *unc-71* transcriptional GFP construct pCZ411, the 1.7 kb upstream regulatory region of *unc-71* was amplified by PCR, and inserted into pPD95.79. For UNC-71::GFP fusion, the GFP-coding sequence from pPD114.35 was inserted at the *Bcl*I site in pCZ418, which resulted in in-frame fusion of GFP in the cytoplasmic region of UNC-71.

Germline transformation was performed following standard procedures (Mello et al., 1991) using 10-20 ng/μl of *unc-71* DNAs and 50-100 ng/μl pRF4 co-injection marker. The P_{unc-71}GFP extrachromosomal arrays were obtained by co-injecting pCZ411 along with the 6.6 kb promoter generated by PCR. One integrant (*juIs166*) of P_{unc-71}GFP extrachromosomal arrays was obtained by a Psoralen-UV induced mutagenesis, and backcrossed multiple times.

To identify lesions in *unc-71* alleles, *unc-71* genomic DNA, including all exons and exon-intron junctions were amplified from *unc-71* mutant and wild-type animals. DNA sequences were determined using ^{33}P labeled primers and the *fmol* sequencing kit (Promega, Madison, WI). All lesions were confirmed on both strands and from DNAs prepared in independent PCRs.

To verify the effect of *ju156* mutation on *unc-71* mRNA, RT-PCR was performed on total RNA isolated from *unc-71(ju156)* animals. Two transcripts were found, one is as predicted by the deletion; the other uses a new splice donor before the deletion. In both transcripts, the reading frame is altered and translation would terminate prior to the metalloprotease domain.

Tissue-specific expression of *unc-71*

The P*unc-115*, P*jam-1*, P*unc-119*, P*unc-33*, P*F25B3.3*, P*unc-25*, P*unc-30* and P*glr-1* promoters (Jin et al., 1994; Hart et al., 1995; Maduro and Pilgrim, 1995; Lundquist et al., 1998; Jin et al., 1999; Altun-Gultekin et al., 2001; Koppen et al., 2001) were inserted upstream of the *unc-71* mini-gene in pCZ418. Other tissue-specific promoters were obtained by PCR amplification to yield fragments that span the following genomic regulatory regions (the numbers indicate

the basepair relative to the ATG): P*twist*, from –1334 to –13; P*sur-5*, from –3711 to –1; P*myo-3*, from –2383 to –1 (Okkema et al., 1993; Harfe et al., 1998; Yochem et al., 1998). The P*e15*2* promoter contains a 234 bp fragment from the *egl-15* promoter region (from –1530 to –1296) that was inserted upstream of the minimal *pes-10* promoter of pPD97.78 (a gift from A. Fire) between the *Hin*dIII and *Stu*I sites. Tissue-specific promoters were inserted into the multiple cloning sites upstream of the *unc-71* minigene in NH#1092. P_{e15*2}*unc-71* was generated by cloning the 5 kb *Spe*I/*Apa*I *unc-71* minigene from NH#1092 into the P*e15*2*-containing construct NH#1134.

Transformation rescue of the SM defects

The *sem-5(n1779)* mutant background was used to reveal the effects of *unc-71* mutations on SM migration. In this background, compromised *unc-71* function causes the animal to have a high-penetrance Egl phenotype and posteriorly displaced SMs. It also significantly enhances the Unc phenotype (Chen et al., 1997). YAC germline transformation rescue was assayed based on the Unc and Egl phenotypes of *unc-71(ay7); sem-5(n1779)*. Transgenic lines were obtained using the co-transformation marker *rol-6(su1006)* in plasmid pRF4. *unc-71* animals attempt to, but cannot complete, the rolling motion. Lines were first scored for rescue of the Unc phenotype; non-Unc lines were then scored for the penetrance of their Egl phenotype.

unc-71 minigenes and constructs where *unc-71* was expressed from tissue-specific promoters were assayed directly for rescue of the posterior SM positioning defect of *unc-71(ju156); sem-5(n1779)* animals. The failure of rescuing the Egl phenotype of this strain by these constructs may be due to multiple egg-laying defects in several cell types that are not rescued by tissue-specific expression of *unc-71* or non-optimal expression of *unc-71* from these transgenic arrays. Most constructs were injected into *unc-71(ay7); sem-5(n1779)* at 50 μg/ml along with pJKL449.1 [P_{myo-2}GFP] at 5 ng/μl; some were injected into *unc-71(ay7); dpy-20(e1282ts); sem-5(n1779)* with pMH86 [*dpy-20(+)*] at 50 ng/μl. The penetrance of the egg-laying defect (%Egl) is scored as the percentage of Egl animals 48 hours after the L4 stage (n>30). SMs are scored with respect to the nuclei of the ventral hypodermal Pn.p cells as described (Thomas et al., 1990).

GFP and motoneuron phenotype analysis

All GFP markers and *unc-71* GFP transgenes were directly observed under a 63× objective on a Zeiss Axioskop fluorescence microscope equipped with a HQ-FITC filter (Chroma, Brattleboro, VT). The type D motoneuron defects were scored using *juIs76* marker as follows. In wild-type L1 animal, the commissures of all six DDs reach the dorsal cord, and DD_1 commissure runs on the left side while the other five on the right side. This pattern was scored as 0% commissure outgrowth defect, 0% circumferential guidance defect and 16.7% (1/6) of LR error. In *unc-71* mutant L1 animals, the commissures that failed to exit the ventral cord were scored as commissure outgrowth defects; the commissures that grew out, but did not reach the dorsal cord, were scored as circumferential guidance defects; and the commissures that run on the opposite sides compared with wild type were scored as LR error. In L2 to adult animals, the same categories were scored for $DD_{2\text{-}6}$ and $VD_{1,3\text{-}13}$. 0% of commissures (0/17) run on the left side in wild-type animals.

RESULTS

unc-71 is *adm-1*

unc-71 was originally defined by one allele, *e541*, isolated by S. Brenner (Brenner, 1974). Twenty additional alleles were isolated in two independent genetic screens: one for mutants with abnormal axon morphology for the type D ventral cord

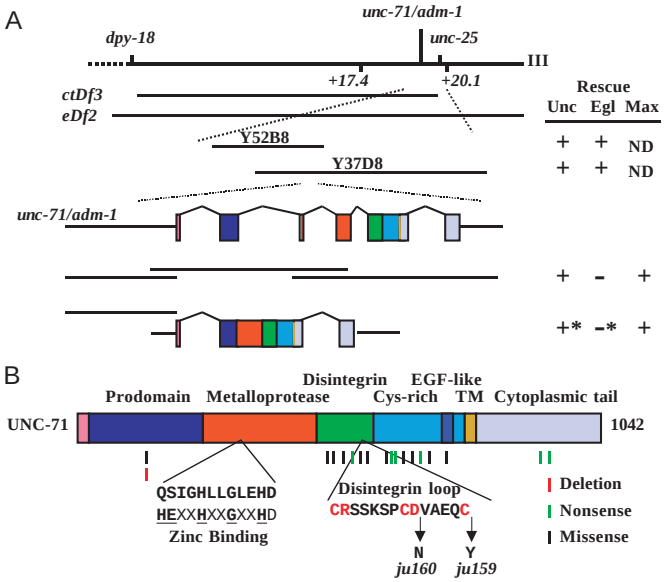

Fig. 1. Cloning of *unc-71*. (A) *unc-71* corresponds to Y37D8A.13/*adm-1*. Rescue of *unc-71* pleiotropies: movement (Unc); egg-laying (Egl); and axon morphology of the D neurons (Max). +, rescue; – no rescue; *, the *unc-71* minigene NH#1092 was used for these experiments. (B) UNC-71 domain structures. UNC-71 contains an inactive metalloprotease domain. A consensus active zinc-binding catalytic site sequence is shown for comparison. The underlined residues are required for zinc binding. The conserved residues in the disintegrin loop are highlighted in red, and lesions of two *unc-71* mutations are shown above. The positions of other *unc-71* mutations are indicated as color-coded bars.

GABAergic motoneurons (Huang et al., 2002), and the other for mutations that enhance the SM migration defects in *sem-5* mutants (Chen et al., 1997). Additional motor axon guidance phenotypes will be described later. All of our alleles are recessive mutations. All the mutants except *ju255* display an uncoordinated phenotype (Unc) that is similar to *e541*, seen as a strong kinker movement, especially when animals move backwards. *ju255* is a weak allele and moves almost indistinguishably from wild-type animals.

unc-71 was previously mapped to the right arm of chromosome III between *dpy-18* and *unc-25*, and is covered by deficiency *tDf6*, but not *ctDf3* (Stein et al., 2001). We further located *unc-71* between SNPs*(III) +17.4* and *+20.1* using the snip-SNP mapping strategy (Wicks et al., 2001) (see Materials and Methods). YAC clones in this region were tested for germline transformation rescue of the severe Unc and egg-laying defective (Egl) phenotypes owing to the *unc-71(ay7)* mutation in a sensitized *sem-5(n1779)* mutant background (Chen et al., 1997). Two overlapping YACs, Y37D8 and Y52B8, were found to rescue both phenotypes of *unc-71(ay7); sem-5(n1779)* (Fig. 1A).

To circumvent the technical difficulty involved in DNA subcloning from YAC clones, we used long-range PCR to amplify DNAs covering each ORF within the region and assessed rescue of the uncoordinated movement and the type D motoneuron axon defects (Max) by germline transformation. One DNA pool that contains three overlapping DNA fragments covering the gene Y37D8A.13 fully rescued both defects of *unc-71(e541)* and *unc-71(ju156)* animals (Fig. 1A).

Y37D8A.13 corresponds to the previously reported *adm-1* gene (Podbilewicz, 1996). We then constructed *unc-71* mini-genes that were expressed from a 1.7 kb *unc-71* promoter (nucleotides –1648 to +61, with the ATG being nucleotides +1 to +3) (see Materials and Methods, and Fig. 1A). When the mini-genes were co-injected with an overlapping 6.6 kb upstream genomic fragment of *unc-71* (nucleotides –6585 to +61), the transgenes rescued *unc-71* mutants to the same extent as the original DNA pool of PCR products (Fig. 1A). Thus, the combination of these two pieces of DNA contains sufficient regulatory and functional sequences of *unc-71*.

unc-71 mutations predominantly affect the disintegrin and cysteine-rich domains

ADM-1 was originally identified from a homology search using conserved sequences of the ADAM family of proteins (Podbilewicz, 1996). It has all the signature domains of ADAM proteins with a relatively long cytoplasmic tail. The metalloprotease domain of ADM-1 is likely to be inactive as it has a glutamine in the first zinc-binding histidine position and a serine in the catalytic residue glutamic acid position (Fig. 1B). The disintegrin loop of ADM-1 has a PCD tripeptide at the position that may correlate to the RGD tripeptide in SVMP (Fig. 1B). Overall, UNC-71/ADM-1 is more closely related to the *mind-meld* gene of *Drosophila* than to other ADAMs, but defines a unique member called ADAM14 (www.gene.ucl.ac.uk/nomenclature/genefamily/metallo.html). Throughout the paper, we refer to this gene as *unc-71*.

To investigate the functional requirement of different domains in the UNC-71 protein, we first determined the molecular lesions in *unc-71* alleles. *ju156* is a 170 bp deletion within the second exon that results in a frameshift followed by a premature stop before the metalloprotease domain (Table 1). Using RT-PCR on RNA isolated from *unc-71(ju156)* mutants, we did not detect any transcripts that would produce functional proteins. Therefore, *ju156* is most probably a null allele of *unc-71*. *ju161* is a missense mutation changing a Gly to an Arg in the prodomain. Most of the lesions in other *unc-71* alleles are clustered in the disintegrin and the cysteine-rich domains (Table 1), providing strong evidence that these two domains are required for UNC-71 function in vivo. More than half of the mutations are missense mutations that might affect specific interactions with binding partners, or protein conformation and stability. Among the six mutations in the disintegrin domain, *ju159* and *ju160* affect two conserved residues in the disintegrin loop, changing Cys509 to Tyr509 and Asp504 to Asn504, respectively (Fig. 1B), supporting a pivotal role of this loop in ADAM proteins. *e541*, *ju157* and *ay47* are three missense mutations in the cysteine-rich domain. *ay44* alters a conserved Cys in the EGF repeat. *ju255*, a weak allele, and *ay48*, a strong allele, both have lesions in the cytoplasmic domain, with *ju255* changing Arg990 to Lys990 and *ay48* generating a stop codon that would delete the last 94 amino acids.

As the metalloprotease domain of UNC-71 is predicted to be inactive and none of our alleles affects this domain, we addressed the functional requirement of this domain by generating an in-frame deletion construct that lacks most of the domain (see Materials and Methods). We found that this construct did not have any *unc-71* rescuing activity in the germline transformation assay (see Table 4B), suggesting that the metalloprotease domain is required for UNC-71 function. It has been shown that GON-1 and MIG-17, both of which share similar protein domain organizations as ADAMs, function as secreted proteins (Blelloch and Kimble, 1999; Nishiwaki et al., 2000). We next explored whether proper membrane localization is necessary for UNC-71 function. We deleted the transmembrane domain and the cytoplasmic tail of UNC-71 (see Materials and Methods). When expressed in *unc-71(ju156)* animals, this construct exhibited no rescuing activity, nor did the transgenes enhance the motor axon defects (see Table 4B). However, when expressed in wild-type animals, this mutant UNC-71 caused a low level of commissure axon choice and aberrant branching in the type D motoneurons, which is similar to, but weaker than, those in *unc-71(ju156)* mutant animals (Table 2; see later). When wild-type *unc-71* was expressed at the similar or higher levels, we did not observe such effects (see Table 4B; Table 2). These results suggest that UNC-71 is required to be anchored in the membrane and that the truncated and likely soluble form of UNC-71 may compete with wild-type protein, possibly by interfering with its interaction with extracellular matrix components.

Based on the identification of the molecular lesions in *unc-71* alleles and the transgene analyses, we conclude that each of the predicted protein functional modules is necessary for UNC-71 function. Moreover, the clustered distribution of *unc-71* mutations in the disintegrin and cysteine-rich domains strongly supports a major function of UNC-71 in regulated cellular adhesion.

Table 1. Molecular lesions of *unc-71* mutants

Allele	Nucleotide change	Amino acid change	Domains
ju161	GGA→AGA	G149R	Prodomain
ju156	170 bp deletion	G149	Prodomain
ay64	GAT→AAT	D461N	Disintegrin
ay46, ay51	CTC→CCC	L471P	Disintegrin
ay17, ad487	TGT→TAT	C477Y	Disintegrin
ay49	CGA→TGA	R490opal	Disintegrin
ju160	GAC→AAC	D504N	Disintegrin
ju159	TGT→TAT	C509Y	Disintegrin
ay45, ay50	CAA→TAA	Q533ochre	Cys rich
ay52	TGG →TGA	W550opal	Cys rich
ju194	GGA→TGA	G551opal	Cys rich
e541	GCG→ACG	A557T	Cys rich
ju157	GGA→GAA	G594E	Cys rich
ay7	CAA→TAA	Q623ochre	Cys rich
ay47	TCG→TTG	S628L	Cys rich
ay44	TGT→AGT	C687S	EGF like
ay48	CCA→CTA	P902L	Cytoplasmic
	CAA→TAA	Q948opal	Cytoplasmic
ju255	AGA→AAA	R990K	Cytoplasmic

ju mutations were isolated in the screen for axon guidance mutants using *juIs76 [P_{unc-25}GFP]* marker (Huang et al., 2002). *ay* mutants were isolated in *sem-5* background (Chen et al., 1997). The underlined letters correspond to the nucleotide alterations. The standard single letter code for each amino acid is used.

The *unc-71* promoter is active in a selected set of cells including the excretory cell and glands, some neuronal and epidermal cells

Antibodies raised against the cytoplasmic domain of ADM-1 detected protein expression in multiple tissues, including

Table 2. Summary of motor axon guidance defects in *unc-71* mutants and transgenes

Genotype	Axon defects				
	Longitudinal defasciculation (penetrance/extent)*	Commissural defects			Vd13 defects‡
		Outgrowth failure†	LR asymmetry	Guidance defects§	
juIs76[P$_{unc-25}$GFP]	<1	0	<1	0	0
unc-71(ju156); juIs76 (L1 larvae)	NA	33	32	21	NA
unc-71(ju156); juIs76	100/36.4	39	39	21	100
unc-71(ju255); juIs76	25/10	6	30	4	70
juIs14[P$_{acr-2}$GFP]	0	0	0	0	NA
unc-71(ju156); juIs14	30/ND	7.1	2.4	3	NA
juIs76; juEx[P$_{unc-115}$UNC-71(ECD)]	0	0	16	0	11
juIs76; juEx[P$_{unc-115}$UNC-71(+)]	0	0	0	0	0

Unless noted, data were collected from 50 young adult animals expressing *juIs76[P$_{unc-25}$GFP]* or *juIs14[P$_{acr-2}$GFP]*.
All data were collected from four or more independent lines.
*% animals exhibiting defasciculation defects/% defasciculated VD neurons
†% commissures that failed to exit the ventral cord in a single animal (divided by 17)
‡Commissures on the left side in a single animal (divided by total number of commissures)
§% commissures that stopped prematurely in a single animal (divided by total number of commissures).
¶The total% of both stalling and U-shaped morphology in VD13.

epidermis, pharynx, vulva and sperm (Podbilewicz, 1996). However, this expression pattern is largely unaltered in *unc-71(e541)* and *unc-71(ju156)* animals, suggesting that the antibodies may recognize an unrelated protein(s) in addition to UNC-71 (B. Podbilewicz, personal communication).

To determine the cell types in which *unc-71* is expressed, we expressed GFP (Chalfie et al., 1994) under the control of the *unc-71* promoter using the combination of the 1.7 kb short promoter along with the 6.6 kb long promoter (see above, and Materials and Methods). GFP expression was first observed in several posterior cells of comma stage embryos, then in the excretory cell and some head neurons in threefold stage embryos (data not shown). In L1 to adult worms, continued expression of GFP was observed in several head neurons, the excretory cell and the excretory gland cells, as well as the sphincter muscles (Fig. 2A-E). We identified one of the head neurons as the AVG neuron based on the cell position and morphology (Fig. 2C). In addition, in L4 worms, GFP was seen in a set of hypodermal cells surrounding the vulva, which persisted in the hypodermal cells flanking the vulval opening in adult worms (Fig. 2E). No GFP expression was detected in the sensory neurons. Faint GFP expression was infrequently detected in one to four neurons in the ventral cord. No expression was observed in the sex myoblasts, nor was GFP detected in the body wall muscles at any stages.

UNC-71 is predicted to be a transmembrane protein. To explore the subcellular localization of UNC-71, we generated a tagged UNC-71::GFP fusion construct by inserting GFP near the end of the cytoplasmic tail (see Materials and Methods). When this construct was expressed under the *unc-115* promoter, it fully rescued the movement and motor axon guidance defects in *unc-71* mutants (see Table 4B; see later). UNC-71::GFP was excluded from cell bodies, and was

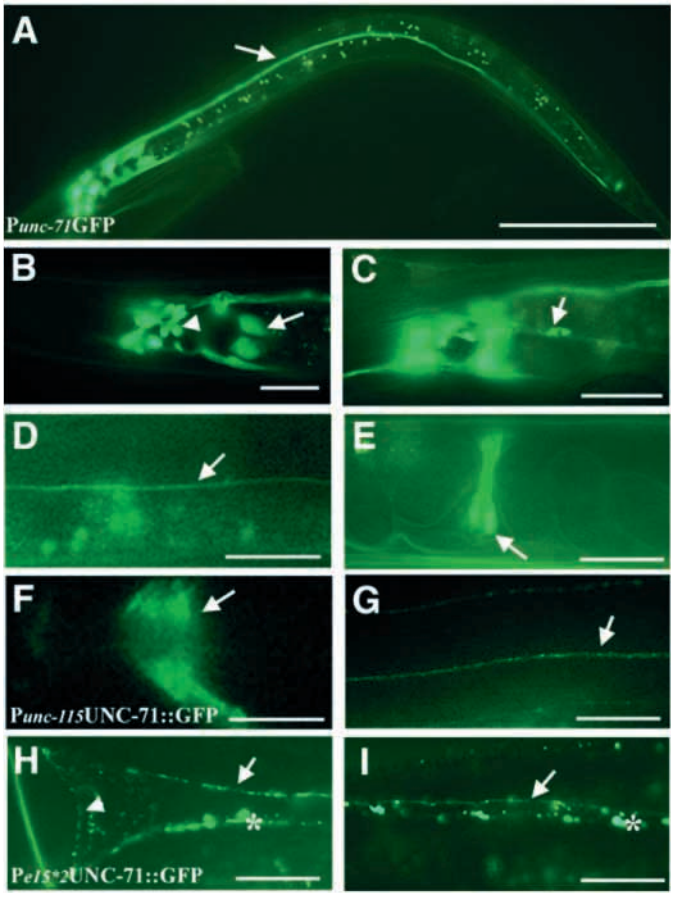

Fig. 2. *unc-71* expression pattern. (A-C,E) Expression patterns of P$_{unc-71}$GFP. GFP is seen in the excretory cell (arrow in A), the excretory gland (arrow in B), in some neurons in the head (arrowhead in B), one of which is AVG interneuron (arrow in C), and in hypodermis (arrow in E) flanking the vulva in adult animals. (D) P$_{unc-71}$GFP is not expressed in the ventral cord motoneurons; the GFP present is from the processes of the interneurons in the head (arrow points to the ventral cord). (F,G) UNC-71::GFP may be localized to the cell membrane. P$_{unc-115}$UNC-71::GFP expression is seen in the nerve ring (arrow in F) and along the nerve cords(arrow in G). (H,I) P$_{e15}$*$_2$UNC-71::GFP expression in hypodermis is seen near the nerve cords (arrow in H,I). Arrowhead in H indicates the vulva hypodermis. *Likely GFP aggregates. Scale bars: 20 μm in A,F-I; 50 μm in B-E.

detected in the areas near the nerve ring (Fig. 2F) and along the nerve cords (Fig. 2G). We also expressed this UNC-71::GFP in hypodermis using the P*e15*2* promoter (see later), and found that GFP was associated to areas near the nerve cord (Fig. 2H,I). Thus, we deduce from the expression pattern of the functional UNC-71::GFP construct that UNC-71 is likely associated with cell membranes.

unc-71 acts cell non-autonomously for sex myoblast migration

The restricted expression pattern of $P_{unc\text{-}71}$GFP raises the question where its function is required for sex myoblast migration and motor axon guidance. We first addressed this question by using a variety of tissue-specific promoters to drive expression of the *unc-71* mini-gene and assaying its function in sex myoblast migration.

unc-71 plays an important role in one of the mechanisms used to guide the migrations of a pair of hermaphrodite sex myoblasts (SMs), the progenitors of the egg-laying muscles (Chen et al., 1997; Chen and Stern, 1998). The SMs migrate anteriorly from the posterior body region to positions that flank the precise center of the gonad (Sulston and Horvitz, 1977). The gonad attracts the SMs to their precise final positions by means of a fibroblast growth factor chemoattractant, a mechanism termed the gonad-dependent attraction (GDA) (Burdine et al., 1998). In the absence of the gonad, the SMs still migrate anteriorly and end up within a range of positions that spans the center of the animal. The mechanism responsible for this movement is known as the gonad-independent mechanism (GIM). Mutations in *unc-71*, as well as in two other genes, *unc-73* and *unc-53*, compromise the GIM (Chen et al., 1997). As long as the gonadal chemoattraction remains, mutations in these genes do not significantly alter the final positions of the SMs. However, when the GDA is compromised, mutations in these genes dramatically affect the ability of the SMs to migrate anteriorly and cause the SMs to remain in severely posteriorly displaced positions. Therefore, to assess the ability of *unc-71* to function in the GIM, a *sem-5* mutant background was used to eliminate the masking effects of the GDA chemoattractive mechanism (Chen et al., 1997).

Although the two YACs containing *unc-71* rescued both the Egl and Unc phenotypes of the *unc-71; sem-5* double mutant, no smaller constructs were found to rescue the Egl phenotype efficiently (Fig. 1A). Therefore, we determined the rescue of the SM migration defect by directly analyzing the distribution of the final positions of SMs in transgenic lines (see Materials and Methods). SM distributions that resembled that of the *sem-5* single mutant were classified as fully rescued, while transgenic lines with distributions resembling the *unc-71; sem-5* double mutant were scored as failing to rescue. Intermediate distributions were classified as showing partial rescue. Examples of these classes of rescue are shown in Table 3A (P*sur-5*, full rescue; P*unc-119*, partial rescue; P*myo-3*, no rescue).

We first tested whether UNC-71 function is permissive or instructive for the guidance of SM migration. For this purpose, the P*sur-5* promoter was used to express UNC-71 in most cells (Yochem et al., 1998). $P_{sur\text{-}5}$*unc-71* was able to fully restore the SM migration function of *unc-71* (Table 3), suggesting that UNC-71 acts permissively to help guide SM migration. Second, to test whether UNC-71 acts within the SMs to guide their migration, *unc-71* was expressed from the *Cetwist* promoter, which drives expression in the SMs (Harfe et al., 1998). P_{twist}*unc-71* showed no rescuing activity, suggesting that UNC-71 probably acts cell non-autonomously to regulate SM migration (Table 3B). Supporting this conclusion, expression of UNC-71 by the P*unc-115* promoter, which drives expression in neurons, the excretory cell and epidermal cells (Lundquist et al., 1998), could fully rescue the SM migration defect in 50% of the transgenic lines (Table 3B). The relatively broad expression pattern of UNC-71 under the control of the P*unc-115* promoter is crucial for effective rescue, as promoters driving more limited tissue-specific expression showed either very weak or no detectable rescue activity. While two fully rescued lines were obtained from hypodermal-specific promoters (P*jam-1* and P*e15*2*), even these were obtained at a very low frequency. Thus, SM or hypodermal expression alone is unlikely to be sufficient to provide UNC-71 activity for SM migration. Interestingly, the overall pattern of promoters that can provide rescuing activity of UNC-71 in SM migration is very similar to that for rescue of the axon morphology defects (see below), suggesting that a crucial UNC-71 expression domain is common to these two different types of cells.

Further examination of axon guidance of DD and VD motoneurons in *unc-71* mutants

Several neuronal defects in *unc-71* mutants have been reported previously (Siddiqui, 1990; Siddiqui and Culotti, 1991; McIntire et al., 1992). To extend these studies, we examined the expression patterns of a panel of GFP markers that visualize either the entire nervous system ($P_{unc\text{-}119}$GFP) or specifically in subsets of neurons, including the touch neurons ($P_{mec\text{-}7}$GFP), the interneurons ($P_{glr\text{-}1}$GFP), the AWC sensory neurons ($P_{str\text{-}2}$GFP), the ventral cord cholinergic motoneurons ($P_{acr\text{-}2}$GFP) and the GABAergic motoneurons ($P_{unc\text{-}25}$GFP). We observed comparable defects in animals homozygous for *ju156, ay7* or *e541*. Overall, longitudinal nerve bundles are mildly defasciculated (Fig. 3I,J), many neurons exhibit low penetrance of premature axon stop and branching errors (10-20% of axons for a given type of neurons, n>50 mutant animals for each GFP marker). For example, 18% of the ASI sensory neurons showed premature stop, and 4% showed axon wander (Fig. 3L). Some neuron cell bodies are occasionally mispositioned (data not shown). A striking differential effect of *unc-71* was observed on the different classes of the ventral cord motoneurons. The cholinergic motoneurons showed less than 10% axon guidance errors (Table 2; see Fig. 5L), whereas the GABAergic type D motoneurons showed fully penetrant defects in several aspects of axon guidance, as described in detail below.

The type D motoneurons include six DD neurons, which are born in the embryo, and 13 VD neurons, which are born at the end of first larval stage (Sulston and Horvitz, 1977; Sulston et al., 1983). Each D neuron first extends a longitudinal process anteriorly along the ventral cord, which then branches out a circumferential process (commissure) growing towards the dorsal cord (see Fig. 3A,C). Upon reaching the dorsal cord, the process bifurcates to elongate both anteriorly and posteriorly (Fig. 3G). The longitudinal processes of each D neuron in both ventral and dorsal nerve cords terminate upon contacting the processes from neighboring neurons of the same class. Therefore, a fully differentiated D neuron has a side-down H-

Table 3. Rescue of the SM migration defects of *unc-71* using tissue-specific promoters

A

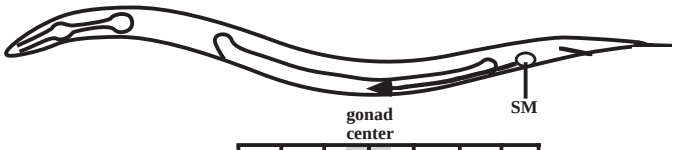

Genotype	Transgene	*n*	% centered SMs	% Egl
sem-5	–	29	55.2	9.1
unc-71(ju156)	–	47	91.5	19.0
unc-71(ju156); sem-5	–	49	13.3	92.6
unc-71(ju156); sem-5; ayEx119	P*sur-5::unc-71*	40	52.8	70.7
unc-71(ju156); sem-5; ayEx120	P*unc-119::unc-71*	41	28.2	73.3
unc-71(ju156); sem-5; ayEx121	P*myo-3::unc-71*	34	17.6	93.8

B

Expression pattern	Transgene promoter	*unc-71* rescuing activity: Full	Partial	None	Total number of lines
Most cells	P*sur-5*	1	0	1	2
Hypodermal cells, neurons and excretory canals	P*unc-115*	2	0	2	4
Hypodermal cells	P*e15*2*	1	0	9	10
Hypodermal cells	P*jam-1*	1	0	5	6
M-lineage	P*twist*	0	0	13	13
Body wall muscle	P*myo-3*	0	0	3	3
Neurons	P*unc-119*	0	1	1	2

All assays for transformation rescue of the SM migration defect were performed in an *unc-71; sem-5(n1779)* background.

(A) Sample SM distributions. The positions of individual SMs are shown by '. Asterisks represent the final positions of non-ventral SMs. Normal and precisely positioned SMs lie within the shaded rectangle. The percent SMs that lie within this region (% centered SMs) are shown for each strain. Although the SM distribution in fully rescued lines can be restored to that of the *sem-5* single mutant, the penetrance of the egg-laying defect (% Egl) is not.

(B) Summary of tissue-specific promoter rescue of the SM migration defect of *unc-71; sem-5* animals. Full rescue, SM distributions similar to *sem-5*; no rescue, SM distributions similar to *unc-71; sem-5* double mutants; partial rescue, intermediate SM distributions. Most of the analyses were performed using *unc-71(ju156)* and the transformation marker *myo-2::GFP*. The P*e15*2* and the P*twist* experiments used *unc-71(ay7); dpy-20(e1282ts); sem-5(n1779)* animals and the transformation marker pMH86[*dpy-20(+)*].

shape (illustrated in Fig. 3K) (White et al., 1986). Strikingly, the commissures from five DDs and 12 VDs exit the ventral cord on the right side of the body, and do not fasciculate (Fig. 3A,C,G). Those from DD_1 and VD_2 exit on the left side and often fasciculate (White et al., 1986). In the ventral and dorsal nerve cords the VD processes fasciculate tightly with those of the DDs (Fig. 3E).

We categorized the axon defects of the type D neurons in *unc-71* mutants into following classes (Table 2, also see Materials and Methods): (1) defasciculation of longitudinal axons (Fig. 3F); (2) failure of commissural outgrowth (Fig. 3D); (3) error in the sidedness of commissures (Fig. 3H); (4) premature stall and wander of commissures (Fig. 3B,H); and (5) abnormal trajectory of the VD13 neuron (Fig. 3K). We collected most of the quantitated data from *unc-71(ju156)* and *unc-71(ju255)* animals, and also made qualitative observations in other strong loss-of-function *unc-71* mutants. In L1 larvae of *unc-71(ju156)*, the ventral longitudinal processes of DD neurons grew to their normal lengths; however, 33% of the DD neuron commissures did not exit the ventral cord (scoring six commissures/animal; *n*=31) (Fig. 3C,D). Of the remaining commissures (average four/animal), 32% run on the left side of the body (range from 0-3, average 1.3), and 21% stopped prematurely before reaching the dorsal cord and wandered in the lateral regions of the body. In L2 to adult mutant animals, the ventral longitudinal nerve bundles of DD and VD neurons were defasciculated (36.4%, scoring 10 VD neurons/animal, *n*=14) (Fig. 3E,F). Thirty-nine percent of all commissures failed to exit the ventral cord (scoring 17 commissures/animal, *n*=43). Of the remaining ones (average 10.6 commissures/animal), 39% run on the left side of the body (range from 1-9, average 4.1), and 21% stopped prematurely and wandered. The failure in commissural growth also left axonal gaps in the dorsal cord; on average, 2.6 axon gaps were seen at various positions in the dorsal cord (Fig. 3G,H). The comparison of the defects in adults with those for DD neurons in L1 larvae indicates that the VD neurons are affected equally as the DDs in *unc-71* mutants. Last, VD13, the most posterior VD neuron,

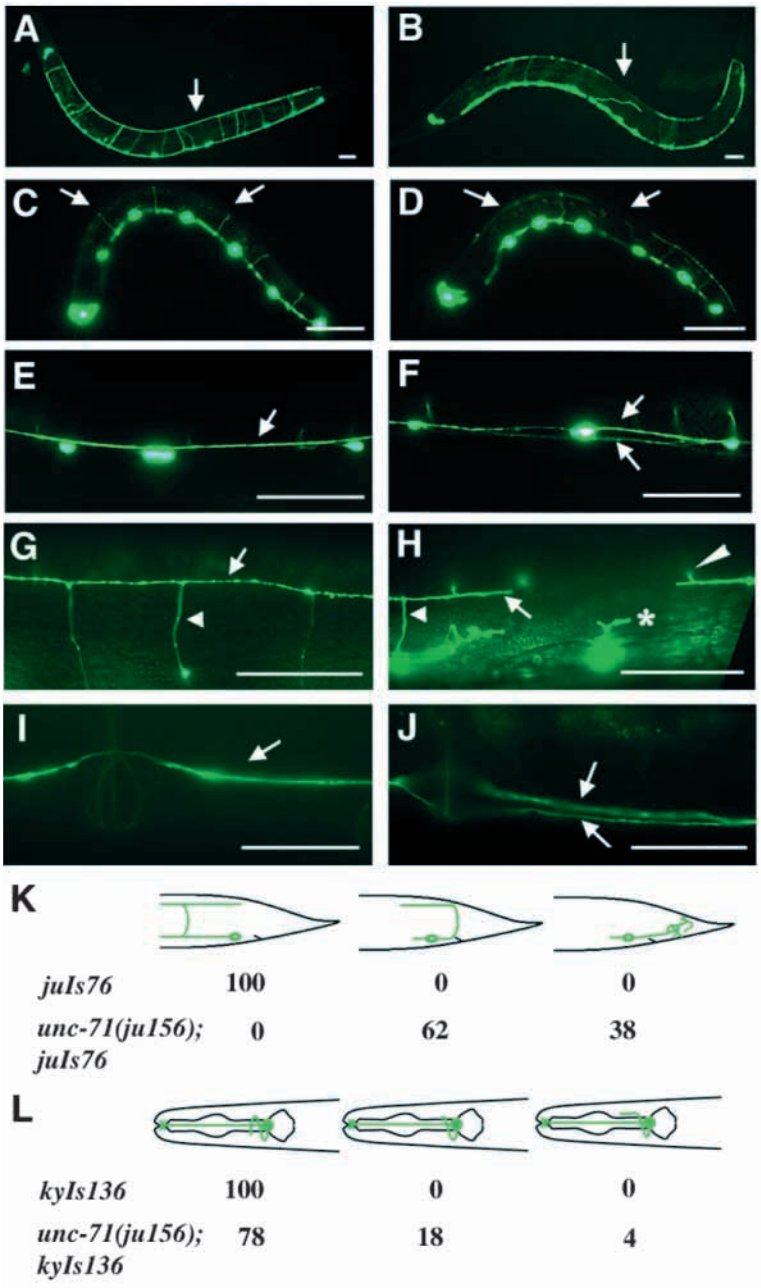

Fig. 3. The type D motoneuron axon guidance defects in *unc-71* mutants. (A-J) Axonal morphology of the type D neurons visualized by *juIs76[P$_{unc-25}$GFP]* marker. (A,B) Low magnification of wild-type (A) and *unc-71* (B) animals. *unc-71* animals have axonal gaps in the dorsal cord (arrows). (C,D) L1 larvae of wild type (C) and *unc-71* (D) animals. Arrows show DD_2 and DD_5 commissures, which did not grow out in *unc-71* animals. (E,F) Ventral views of wild-type (E) and *unc-71* (F) animals. In wild-type animals, DD and VD ventral processes form a tight bundle (arrow in E); in *unc-71* animals, defasciculation is seen as two separated bundles (arrow in F). (G,H) Dorsal views of wild-type (G) and *unc-71* (H) animals. (G) All commissures (arrowhead) reach the dorsal cord (arrow) from the same side in wild-type animals. (H) In *unc-71* animals, commissures (arrowheads) reach the dorsal cord (arrow) from both sides (left side, narrow arrowhead; right side, arrowhead) and some do not reach the dorsal cord (asterisk). (I,J) Ventral view of wild-type and *unc-71* animals expressing *nuIs25[P$_{glr-1}$GFP]* in the interneurons. In wild-type animals, the ventral cord processes of these interneurons form a tight bundle (arrow in I); in *unc-71* they are defasciculated (arrow in J). (K,L) Schematics of VD_{13} neuron morphology viewed using *juIs76* marker (K) and AWC neuron morphology viewed by *kyIs136[P$_{str-2}$GFP]* marker (L) in wild-type and *unc-71* animals. Numbers represent the percentage of particular phenotypes. Scale bars: 20 μm in C,D; 50 μm in A,B,E-J.

showed distinct defects in that instead of sending a process anteriorly, it always sent out a process posteriorly, which either stalled and extended numerous branches in the tail (38%, *n*=63), or grew dorsally to join the dorsal cord where it looped back extending anteriorly and forming a left-side-down U shape (62%) (Fig. 3K).

In the weak allele *unc-71(ju255)* animals, the major defects were seen in VD13 trajectory and in the sidedness choice for commissures (Table 2). Ninety-four percent of the commissures exited the ventral cord, 30% of which run on the left side, and only 4% did not reach the dorsal cord (*n*=30). The phenotypes in *ju255* suggest that the decision of the growth cones at the commissural exit choice is more sensitive to *unc-71* activity than those for longitudinal axon fasciculation and circumferential growth.

unc-71 acts cell non-autonomously to regulate D motor neuron axon guidance

To address where UNC-71 function is required for D neuron axon guidance, we first performed genetic mosaic analysis with *unc-71(ju156); juIs76[P$_{unc-25}$GFP]* animals that also carried an extrachromosomal array containing the *unc-71* rescuing DNA pool and SUR-5::GFP, a cell-autonomous nuclear GFP marker (Yochem et al., 1998). The AB lineage generates neurons and hypodermis, and the P1 lineage produces all but one muscle (Sulston et al., 1983). We found eight mosaic animals that lost the *unc-71(+)* array in the AB, but not the P1, lineage, and all eight animals exhibited axon defects in the D neurons. By contrast, 10 animals that lost the array in the P1, but not the AB, lineage showed wild-type axon morphology of the D neurons. This analysis indicates that *unc-71* function is required in the neuro-hypodermal lineage for motor axon guidance. Consistently, when *unc-71* was expressed from the *unc-115* promoter (Lundquist et al., 1998), it fully rescued the D neuron axon phenotypes (Table 4).

In which cells of AB lineage does *unc-71* act? We expressed *unc-71* pan-neurally using three promoters: P*unc-119* (Maduro and Pilgrim, 1995), P*unc-33* and PF25B3.3 (Altun-Gultekin et al., 2001) and observed a partial rescue of the D neuron axon defects (Table 4A). We also expressed *unc-71* in all epidermal cells using the P*e15*2* promoter, and observed similar rescuing activity. By contrast, expression of *unc-71* from the *myo-3* muscle promoter (Okkema et al., 1993) did not show any rescuing activity. These data further support that *unc-71* function is required in both neurons and epidermis for motor axon guidance.

In which neurons does *unc-71* act? We expressed *unc-71* specifically in the D neurons using the *unc-30* or *unc-25*

Table 4. UNC-71 functions cell non-autonomously in D neuron axon guidance

A

Tissue and cell types	Transgene promoter	Rescuing activity of Max phenotypes* +++ (0-10%)	++ (10-20%)	+ (20-40%)	No rescue (>40%)
Hypodermal cells, neurons and excretory canal cells	P*unc-115*	3	0	2	0
Hypodermal cells	P*e15*2*	0	0	4	1
Neurons	P*unc-119*†	0	0	3	2
Neurons	P*unc-33*	0	2	3	1
Neurons	P*F25B3.3*	0	1	2	2
Interneurons	P*glr-1*	0	0	2	6
D neurons	P*unc-25*†	0	0	0	9
D neurons	P*unc-30*	0	0	0	3
Body wall muscles	P*myo-3*	0	0	0	5

B

Constructs	Rescuing activity of Max phenotypes* +++ (0-10%)	++ (10-20%)	+ (20-40%)	No rescue (>40%)
$P_{unc-115}$-UNC-71	3	0	2	0
$P_{unc-115}$-UNC-71::GFP	1	3	0	0
P_{e15*2}-UNC-71	0	0	4	1
P_{e15*2}-UNC-71::GFP	0	1	3	0
$P_{unc-115}$-UNC-71(M^-)	0	0	0	6
$P_{unc-115}$-UNC-71(ECD)†	0	0	0	4
P_{unc-71}-UNC-71†	5	2	2	10

(A) Rescue of *unc-71(ju156)* D neuron axonal defects by tissue specific promoters driving the *unc-71* minigene.

*Degree of rescue is represented by % axon dorsal guidance defects. The dorsal guidance defects of the D neuron axons, visualized by *juIs76*, were quantified by counting the number of commissures from $DD_{2\text{-}6}$ and $VD_{1,3\text{-}13}$ that did not reach the dorsal cord within a single animal, which was then divided by 17 to convert to the percentage of defects.

unc-71(ju156) animals display 48±8% axon guidance defects, scored as 'no rescue'.

(B) Functional analysis of UNC-71. UNC-71(M^-), metalloprotease domain deletion construct; UNC-71(ECD), extracellular domains of UNC-71 only. Twenty to 50 animals were scored for each transgenic line, and the average percentage was presented.

†DNAs were injected at 20 ng/μl and 100 ng/μl, and the results were similar. Only the results from the 20 ng/μl DNA injection are presented.

promoter (Jin et al., 1994; Jin et al., 1999), and found that neither transgenes rescued the axon defects (Table 4), indicating that *unc-71* may act in other neurons to control D neuron axon guidance. Expression of *unc-71* in cholinergic ventral cord motoneurons using the *acr-2* promoter did not rescue the D neuron axon defects. By contrast, expression of *unc-71* from the *glr-1* promoter, which is active in several interneurons including the AVG neuron (Hart et al., 1995), partially rescued the axon defects of the D neurons in *unc-71* mutants to the same extent as $P_{unc-119}$ UNC-71 (Table 4A). *unc-71* is expressed in AVG (Fig. 2C). We do not rule out that the expression of *unc-71* in other *glr-1*-expressing neurons contributes to guide the D neuron axons. Nonetheless, these data support the conclusion that *unc-71* functions cell non-autonomously for motoneuron axon guidance, and suggest that one possible neuronal source of UNC-71 is from the AVG neuron.

Genetic interactions of UNC-71 with other ADAMs indicate that UNC-71 does not act through other active ADAMs

It has been suggested that an ADAM protein with an inactive metalloprotease domain could function as an endogenous inhibitor to regulate the activity of an ADAM with an active metalloprotease (Pan and Rubin, 1997). The *C. elegans* genome has four ADAMs (The *C. elegans* Genome Consortium, 1998). Except for UNC-71, the other three ADAMs (ADM-2, SUP-17 and ADM-4) all contain active catalytic site sequences in their metalloprotease domains (Wen et al., 1997) (B. Podbilewicz, personal communication; this study). If *unc-71* acts as an inhibitor for these active ADAMs, we would expect that some of the phenotypes in *unc-71* might be due to hyperactive metalloprotease activities of the other ADAMs, and therefore, could be suppressed by eliminating or reducing the function of these active ADAMs.

We first examined the D neuron morphology in the other ADAM mutants. Animals homozygous for *adm-2(tm347)* or *adm-4(ok265)*, both of which are deletion mutations (see Materials and Methods), are viable, fertile, have no obvious behavioral defects, and show no defects in D neuron morphology (Fig. 4A). *sup-17(n1258ts)* is a temperature-sensitive mutation, and the animals are viable at 15-22.5°C, but lethal at 25°C. In *sup-17(n1258ts)* animals cultured at 22.5°C, we observed a very weak D neuron axon guidance defect such that about 4% of the commissures failed to reach the dorsal cord (Fig. 4A).

We then constructed double mutants between *unc-71* and mutations in the other ADM genes, and observed no suppression in any of the double mutants (Fig. 4A). Both *unc-71(ju156); adm-2(tm347)* and *unc-71(ju156); adm-4(ok265)* double mutants showed phenotypes indistinguishable from that of the *unc-71(ju156)* single mutant (Fig. 4A). *sup-17(n1258ts);*

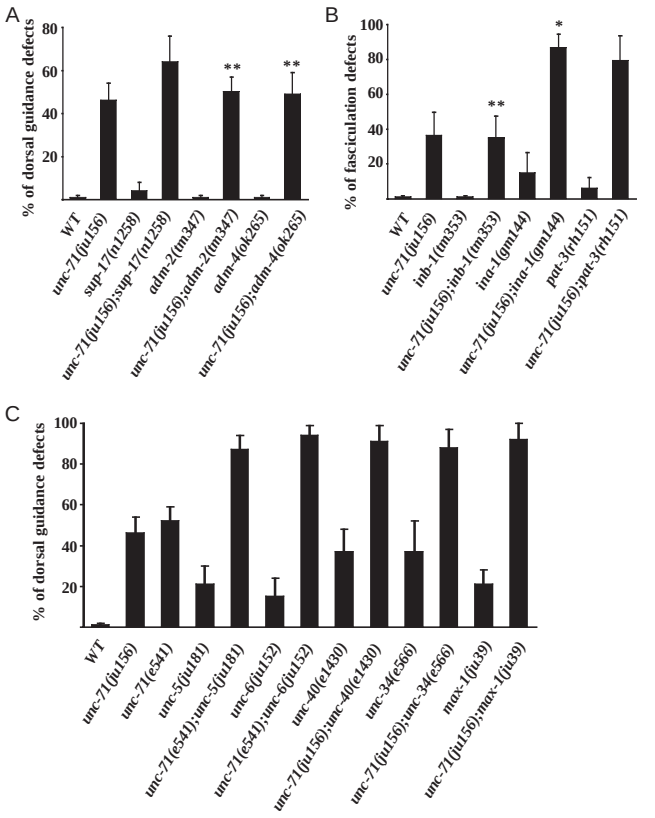

Fig. 4. Genetic interactions of *unc-71* with ADAMs, integrins, *unc-6* and other signaling molecules. (A) *unc-71* acts independently of the other three *C. elegans* ADAMs. Percentages of dorsal guidance defects were quantified as Table 4. (B) Axonal fasciculation defects in *unc-71* were strongly enhanced by mutations in *ina-1* and *pat-3* but not *inb-1*. The percentages of fasciculation defects were quantified by counting the number of ventral cord processes from VD_{3-12} that were separated from the DD ventral cord processes, divided by 10. (C) Axonal defects in double mutants of *unc-71* with mutants in the *unc-6/netrin* signaling pathway. Percentages of dorsal guidance defects were quantified as Table 4. Bars represent standard deviation. **P*<0.001, Student's *t*-test, compared with *unc-71* single mutant control. ***P*>0.05, Student's t-test, compared with *unc-71* single mutant control.

unc-71(ju156) double mutants raised at 22.5°C showed slightly enhanced axon guidance defects: 64% of the commissures failed to reach the dorsal cord compared with 48% and 4% in *unc-71(ju156)* and *sup-17(n1258ts)* single mutants, respectively (Fig. 4A). From these analyses, we conclude that *unc-71* is unlikely to act through the other three ADAMs.

unc-71 acts in parallel to *ina-1*/*pat-3* integrins in motor axon guidance

It is generally thought that a major function of ADAM proteins is to regulate the extracellular matrix, and that the integrin receptors are important targets of ADAM proteins (Wolfsberg et al., 1995; Evans, 2001). The *C. elegans* genome has two integrin-α subunits, *ina-1* and *pat-2*; one integrin-β subunit, *pat-3*; and one integrin-β subunit, *inb-1* (Hutter et al., 2000). INA-1 can form a protein complex with PAT-3, and is expressed and functions cell-autonomously in neurons and migrating cells (Baum and Garriga, 1997). The *ina-1*-null mutants are L1 lethal, and exhibit weak defasciculation and commissural outgrowth defects in the D neurons (Baum and Garriga, 1997) (Fig. 4B). *pat-2* and *pat-3* are reported to be expressed predominantly in muscles and gonad, and may form a complex (Williams and Waterston, 1994; Gettner et al., 1995). Null mutants of *pat-2* or *pat-3* are arrested as paralyzed twofold stage embryos (Williams and Waterston, 1994), precluding us from determining the neuronal phenotypes in these animals. In partial loss-of-function mutation *pat-3*(*rh151)* animals, we observed that the D neurons displayed a low level of defasciculation and commissure outgrowth defects (Fig. 4B). Similar defects have also been reported by a study using *pat-3* RNAi (Poinat et al., 2002). INB-1 is a rather divergent member of integrins. The *inb-1(tm353)* mutants, a likely knockout mutation (see Materials and Methods), are viable, fertile, have no obvious behavior defects and their D neuron morphology is normal (Fig. 4B).

To investigate how *unc-71* interacts with the *C. elegans* integrins, we made double mutants of *unc-71* with viable alleles of these integrins. *inb-1(tm353); unc-71(ju156)* double mutants showed similar axon defects as *unc-71(ju156)* alone (Fig. 4B), suggesting that *inb-1* acts in a separate process from *unc-71*. By contrast, *unc-71* showed synergistic interactions with *ina-1* and *pat-3* in longitudinal axon fasciculation. For example, in adult animals of *ina-1(gm144)*, 15% of the longitudinal processes of D neurons showed defasciculation (scoring 10 VD neurons/animal, *n*=15), about 16% of the commissures run on the left side, but most commissures reached the dorsal cord (98%, 17 commissures/animal, *n*=27) (Fig. 4B) (Baum and Garriga, 1997). Although *gm144* is a partial loss-of-function mutation of *ina-1* (Baum and Garriga, 1997), the axon defects of the DD neurons in L1 larvae of *ina-1(gm144)* were comparable with those of *gm86* (data not shown), a null allele of *ina-1*, suggesting that the D neuron phenotypes we scored here reflect the null phenotypes of *ina-1* in these neurons. In the *unc-71(ju156); ina-1(gm144)* double mutants, the ventral fascicle of the D neurons were severely disorganized (Fig. 5J): 90% of the longitudinal D axon bundles were defasciculated (10 VD neurons/animal, *n*=18), compared with 37% and 15% for *unc-71(ju156)* and *ina-1(gm144)* alone. Likewise, 80% of the D neurons showed defasciculation in *unc-71(ju156); pat-3(rh151)* animals, compared with 37% and 6% for *unc-71(ju156)* and *pat-3(rh151)* alone. In addition, greater number of commissures failed to reach the dorsal cord in these double mutants than each single mutant (Fig. 5D). The phenotypic similarities in *unc-71; ina-1* and *unc-71; pat-3* double mutants lend further support for the hypothesis that INA-1 and PAT-3 are functional partners in vivo. Moreover, the enhanced defects in the double mutants of *unc-71* with *ina-1* or *pat-3* suggest that *unc-71* is unlikely to act through *ina-1/pat-3* integrins; rather, it acts redundantly, or in parallel to, *ina-1/pat-3* to control axon fasciculation.

unc-71 likely acts in parallel to netrin-induced axon repulsion

It has been shown that chemical inhibitors of metalloproteases can potentiate netrin-mediated axon outgrowth and guidance, and the netrin receptor DCC appears to be a substrate for metalloprotease-dependent ectodomain shedding (Galko and Tessier-Lavigne, 2000). Drosophila *kuz* mutants exhibit axon

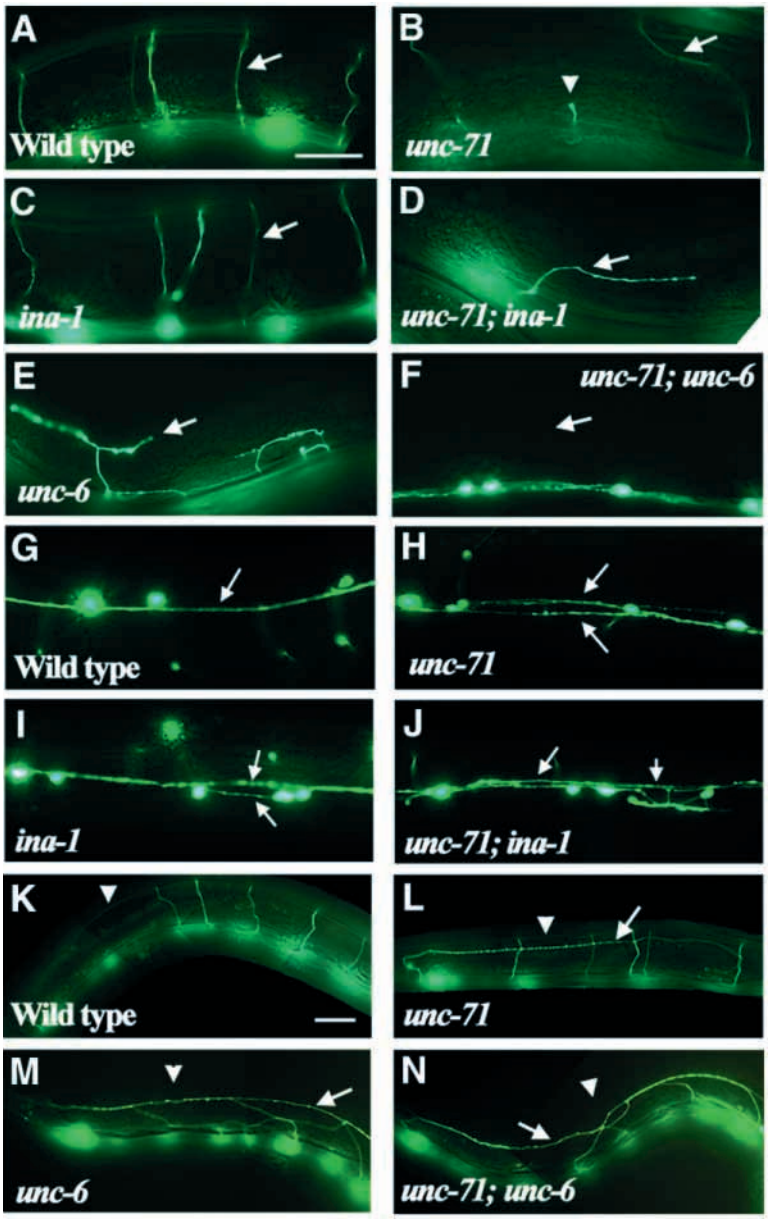

Fig. 5. Axon guidance phenotypes in the double mutants. (A-F) Lateral view of *juIs76[P$_{unc-25}$GFP]* in different genetic backgrounds. In wild type (A) and *ina-1(gm144)* (C) animals commissures (arrow) all reach the dorsal cord. In *unc-71*, fewer commissures (arrow) grow out and some stop short (arrowhead in B). (D) In *unc-71(ju156); ina-1(gm144)* animals, even fewer commissures (arrow) grow out. (E) In *unc-6(ev400)* animals, few commissures (arrow) grow out but all are defective. (F) In *unc-71(ju156); unc-6(ev400)* animals, no commissures grow out of the ventral cord. Arrow indicates the lateral positions where commissures would be found in *unc-6* mutants. (G-J) Ventral view of *juIs76* in different genetic backgrounds. (G) DD and VD ventral processes are fasciculated forming a tight bundle (arrow) in wild-type animals. (H,I) DD and VD ventral processes are defasciculated in *unc-71(ju156)* and *ina-1(gm144)* animals as two separated processes (arrow). (J) The ventral cord (arrows) is largely disorganized in *unc-71(ju156); ina-1(gm144)* animals. (K-N) DA and DB motoneurons in different genetic backgrounds viewed by *juIs14[P$_{acr-2}$GFP]*. In wild type, all commissures reach the dorsal cord (arrowhead in K); in *unc-71(ju156)* occasionally one commissure does not reach the dorsal cord (arrowhead) but instead runs laterally (arrow in L); in *unc-6(ev400)* none of the commissures reaches the dorsal cord (arrowhead in M) and all run laterally (arrow in M); in *unc-71(ju156); unc-6(ev400)* double mutants none of the commissures reaches the dorsal cord (arrowhead) and all run laterally (arrow in N), which is similar to *unc-6* alone (M). Scale bars: in A, 50 μm for A-J; in K, 50 μm for K-N.

extension defects, the mechanism for which is not known (Fambrough et al., 1996). The circumferential guidance of D neuron commissures is repelled by the UNC-6/netrin. UNC-6 acts upon the UNC-5 receptor and the UNC-5 and UNC-40/DCC co-receptor (Wadsworth, 2002). The signal transduction pathway downstream of the receptors is in part mediated by *unc-34/Ena* and *max-1* (Colavita and Culotti, 1998; Huang et al., 2002). In mutants for each of these genes, the circumferential axon guidance of D neurons is disrupted to different extents (Hedgecock et al., 1990; McIntire et al., 1992; Colavita and Culotti, 1998; Huang et al., 2002). To explore potential interactions between *unc-71* with *unc-6*/netrin signaling pathway, we conducted double mutant analysis as below.

In null mutants for *unc*-6 or *unc-5*, about 35% or 26% of the D neuron commissures grew out of the ventral cord, respectively; but none reached the dorsal nerve cord. In *unc-71(ju156)* animals, 61% of the D neuron commissures grew out of the ventral cord, of which 21% failed to reach the dorsal nerve cord. In both *unc-71(ju156); unc-5(e53)* and *unc-71(ju156); unc-6(ev400)* double mutants, no commissures of the D neurons grew out of the ventral cord (Fig. 5F). Moreover, this complete block of commissural outgrowth in the double mutants is specific to the type D neurons because the commissural outgrowth and guidance of the DA and DB motoneurons, which also depends on *unc-6* and *unc-5* (Hedgecock et al., 1990), was comparable between the double mutant animals and *unc-5* or *unc-6* single mutants alone (Fig. 5M,N). These observations indicate that *unc-71* and *unc-6* act in parallel to control commissural outgrowth.

To examine how *unc-71* interacts with the *unc-6/netrin* signaling pathway in circumferential axon guidance, we used partial loss-of-function mutations of *unc-5* and *unc-6*. In these animals, all D neuron commissures exit the ventral nerve cord, and only a fraction of them exhibited circumferential guidance defects; for example, 21% and 15% for *unc-5(ju181)* and *unc-6(ju152)*, respectively (Fig. 4C). In *unc-71(e541)*; *unc-5(ju181)* and *unc-71(e541)*; *unc-6(ju152)* double mutants, however, the circumferential guidance defects were strongly enhanced to 87% and 90%, respectively (Fig. 4C). Similar enhancement was also observed for double mutants between *unc-71* with *unc-40*, or *unc-34*, or *max-1* (Fig. 4C). We also noticed that the final positions of the stalled growth cones in the double mutants resembled those in the netrin signaling mutants more than those in *unc-71* mutants. For example, in *unc-71(ju156 or e541)* single mutants, most stalled growth cones were found within the dorsal half along the side of the

worm, whereas in *unc-5(ju181)* and *unc-5(ju181); unc-71(ju156)* double mutants, the growth cones were stalled at various positions along the dorsoventral axis. Similarly, the stalled growth cones were often found at mid-lateral range along the dorsoventral axis for *unc-40(e1430)* and *unc-40(e1430); unc-71(ju156)* double mutants, and at ventral half in *max-1(ju39)* and *max-1(ju39); unc-71(ju156)* double mutants. Because the double mutants between *unc-71* with netrin signaling molecules all showed an overall additivity to enhancement, we interpret these results to mean that *unc-71* functions in parallel to netrin-mediated commissural outgrowth and circumferential guidance. However, the observation that the final positions of the stalled growth cones in the double mutants resemble those of netrin signaling pathway mutants alone may imply that *unc-71* modulates the cellular motility of growth cones through events downstream of netrin receptors.

DISCUSSION

Cell migration and growth cone navigation require constant dialogue between migrating cells or growth cones and their environments. The ADAM proteins have been implicated in cell-cell adhesion or recognition in diverse cellular processes, including cell migration, cell fusion and organ formation (Bigler et al., 1997; Primakoff and Myles, 2000; Lieber et al., 2002; Seals and Courtneidge, 2003). We have demonstrated that the *C. elegans* UNC-71 ADAM protein functions in a cell non-autonomous manner to control distinct aspects of motoneuron axon guidance and sex myoblast migration. The cell adhesion domains of UNC-71 are particularly crucial for its function. Genetic double mutant analysis of *unc-71* with other axon guidance signaling molecules suggests that UNC-71 probably functions in a combinatorial manner with integrins and UNC-6/netrin to provide distinct axon guidance cues at specific choice points for motoneurons.

A crucial function of UNC-71 is in cell adhesion

The ADAM proteins are composed of multiple protein functional modules. Current studies of ADAMs have focused on the metalloprotease and the disintegrin domains. Our analysis of the many alleles of *unc-71* and transgene studies provides a comprehensive in vivo examination of the structural and functional correlation of an ADAM protein.

On the basis of the sequence comparison, UNC-71 is unlikely to be an active metalloprotease (Fig. 1A) (Podbilewicz, 1996). We find that none of the large number of existing *unc-71* mutations has missense mutations in this domain. However, deletion of this domain abolishes UNC-71 rescuing activity. It has been shown that the metalloprotease domain of MIG-17 is required for MIG-17 localization (Nishiwaki et al., 2000). It is possible that the inactive protease domain of UNC-71 may be necessary for maintaining the structural integrity, or for facilitating post-translational processing for proper targeting of the protein.

An important finding of our mutation analysis is that the majority of *unc-71* mutations are missense mutations altering conserved residues in the disintegrin and cysteine-rich domains, lending strong support to the hypothesis that these domains are important functional modules. In particular, in vitro studies have indicated the importance of an aspartic acid residue in the disintegrin loop of ADAMs for their interactions with integrins (Zhu et al., 2000). We find that the *ju160* mutation alters this Asp residue, and behaves as a null mutation. The observation that expression of the extracellular region of UNC-71 in wild-type animals weakly phenocopies the axon guidance defects seen with partial loss-of-function mutations of *unc-71* is also consistent with the notion that UNC-71 is involved in a regulated cellular adhesion process. Based on the lesions in *unc-71* loss-of-function mutations, we believe that a crucial role of UNC-71 is in cell adhesion.

unc-71 acts cell non-autonomously in D neuron axon guidance and sex myoblast migration

Although UNC-71 appears to be expressed as a membrane protein and the membrane anchorage is necessary to control its activity, we have substantial evidence to support the conclusion that *unc-71* functions in a cell non-autonomous manner for motoneuron axon guidance and SM migration. First, *unc-71* shows restricted expression in a selected set of cells that do not appear to include the motoneurons and sex myoblasts. Second, expression of UNC-71 in the D neurons alone does not rescue the axon guidance defects; nor does expression of UNC-71 in muscles rescue the migration defects of sex myoblast. Third, our tissue-specific expression and rescue study shows that the motoneuron axon guidance and SM migration depend on the expression of *unc-71* in epidermis and neurons. A cell non-autonomous function is not unusual for membrane-anchored proteins. For example, Kuz has both cell-autonomous and cell-non-autonomous roles in bristle development (Rooke et al., 1996). Ephrins are known to function cell non-autonomously in neuron for epidermal cell migration in *C. elegans* (George et al., 1998). In light of the cell non-autonomous requirement for *unc-71*, it is somewhat surprising to find that *unc-71* mutations cause profound defects in the type D neurons without significant effects on the other types of the ventral cord motoneurons, despite that these neurons are born within close proximity and migrate along nearly identical paths. This observation suggests that UNC-71 does not alter the extracellular matrix in a global manner; rather, UNC-71 interacts with a receptor(s), or alters the distribution of a ligand(s) for a receptor(s) on the type D neurons.

The molecular identification of UNC-71 as an ADAM metalloprotease and the possibility that it acts in a cell non-autonomous manner in SM migration is an important step forward in understanding the control of SM migration guidance by the gonad-independent mechanism (GIM). Little is known about the source of guidance information for this mechanism. Three components of this mechanism have been identified: UNC-53, UNC-73 and UNC-71 (Chen et al., 1997). Double mutant combinations between any of the three genes *unc-71*, *unc-73* and *unc-53* have SM distributions that are essentially wild type and similar to the single mutants (E. Chen and M.J.S., unpublished), consistent with these components acting in a single pathway that mediates the GIM. Both UNC-53 and UNC-73 encode proteins containing structural domains or activities that can modify the intracellular cytoskeleton, and they have cell-autonomous function in other processes (Steven et al., 1998; Stringham et al., 2002). A cell non-autonomous role for UNC-71 in SM migration provides a link to the extracellular cues involved in the gonad-independent mechanism.

UNC-71 provides dynamic and distinct guidance cues for D motor axons

Precise axon trajectory is achieved in a stepping stone manner, and growth cones can detect specific guidance information at specific choice points or guideposts (Tessier-Lavigne and Goodman, 1996). The *C. elegans* type D neurons have at least four guideposts during their axon trajectory: longitudinal fasciculation, branching of circumferential processes, circumferential guidance and bifurcation in the dorsal cord. Mutations in several genes have been shown to affect one guidance aspect predominantly. For example, *ina-1* regulates the longitudinal fasciculation (Baum and Garriga, 1997); the UNC-6/netrin and its receptors UNC-5 and UNC-40 regulate the dorsal-directed commissural growth (Wadsworth, 2002). In *unc-71* mutants, we find a range of axon guidance defects that are consistent with an interpretation that *unc-71* is required in three steps, with a major function in longitudinal fasciculation and commissural branching, and a minor role in dorsal-directed guidance.

Axon fasciculation requires cell-cell interactions and is generally thought to be mediated by short-range or contact-mediated guidance mechanisms. A prominent defect of *unc-71* mutants is defasciculation of the DD and VD longitudinal processes. ADAM proteins are implicated in promoting cellular adhesion mostly through the integrin receptors (Evans, 2001). Integrins function as αβ heterodimer receptors (Miranti and Brugge, 2002). In *C. elegans*, PAT-3/β-integrin can form dimers with INA-1 or PAT-2 α integrins (Baum and Garriga, 1997; Gettner et al., 1995). We could not address the interaction of *unc-71* with *pat-2* for the early lethality of *pat-2* null mutants and for the lack of viable alleles. The fasciculation defects in *ina-1* and *pat-3* mutants are much weaker than those in *unc-71*, and are strongly enhanced in *ina-1; unc-71* and *pat-3; unc-71* double mutants. These observations are consistent with a conclusion that UNC-71 does not act through these integrins; rather, it acts independently of, or in parallel to, *ina-1/pat-3* integrins in axon fasciculation.

The second guidepost for the D neurons is the branch choice of the circumferential processes. In wild-type animals, the D neurons extend side branches near the anterior end of the ventral processes, and there is a striking asymmetry in that 17 out of the 19 commissures exit to the right side of the animal. In *unc-71* mutants, 39% of the branches fail to exit the ventral cord, and 39% of the remaining ones choose the left side. This branching defect is an unlikely secondary consequence caused by the defasciculation defects of the ventral processes, because *unc-71(ju255)* specifically disrupts the branch sidedness decision without affecting fasciculation. Moreover, mutations in *unc-5* and *unc-40* cause defasciculation of the ventral processes, but do not affect the asymmetrical preferences of the commissural branches (Hedgecock et al., 1990; McIntire et al., 1992) (this study). Thus, the activity of UNC-71 appears to be more crucial for the branch choice than for longitudinal fasciculation. It has been shown that killing the AVG neuron, which projects a long process to pioneer the ventral cord and fasciculates with the extending D processes, causes the branches of the D neurons to exit to the left side (R. Durbin, PhD Thesis, University of Cambridge, 1987). We find that *unc-71* is expressed in AVG and that the axon defects of the D neurons can be partially rescued by expressing UNC-71 from the *glr-1* promoter. These data support the hypothesis that UNC-71 expressed from the AVG neuron may facilitate a localized guidance source at the D neuron branch points. AVG also expresses UNC-6 (Wadsworth et al., 1996), and *unc-6* mutants show commissural outgrowth failure and LR sidedness errors (Hedgecock et al., 1990) (this study). We find that in *unc-71; unc-6* and *unc-71; unc-5* double null mutants the commissural outgrowth is completely blocked, indicating that UNC-71 acts in parallel to UNC-6 and UNC-5. *ina-1* mutants show LR sidedness errors (Baum and Garriga, 1997); however, the commissural outgrowth defects in *unc-71; ina-1* double mutants are the same as in *unc-71* mutant alone. Conceivably, UNC-71 may create a microdomain at the commissural exit guidepost to facilitate the combinatorial interactions between these molecules.

The third guidepost for the D neurons is the dorsal-directed migration of the commissures. UNC-6 provides a long-range repulsive cue, and acts through its receptors UNC-5 and UNC-40 (Wadsworth, 2002). Both the *unc-71* mutant phenotypes and the double mutant analysis of *unc-71* with genes involved in this UNC-6 repulsion pathway indicate that *unc-71* modulates this axon guidance process. Although ectodomain shedding of netrin receptors and other transmembrane receptors by ADAMs have been implicated in growth cone movement (Fambrough et al., 1996; Galko and Tessier-Lavigne, 2000), we think that it is unlikely the mechanism for UNC-71 because of the absence of an active protease site and the predominant association of mutations in the domains involved in cell adhesion. Different from the longitudinal elongation and commissural branching that depend on the interactions between the D neuron growth cones with epidermis and other neurons, the commissures migrate through a solely epidermal substrate. We therefore propose that UNC-71 expressed from the epidermal cells modifies the extracellular matrix to provide an independent, short-range, permissive guidance cue for the D growth cones.

Our expression and functional studies show that UNC-71 appears to be produced globally from multiple sources. It is therefore surprising to find that *unc-71* has a striking differential effect on the axon guidance of neurons that migrate along similar path. For example, the circumferential guidance of DA and DB neurons uses similar guidance information provided by the UNC-6 repulsion pathway (Hedgecock et al., 1990), and *ina-1* modulates longitudinal axon fasciculation for all ventral cord neurons (Baum and Garriga, 1997) (X.H. and Y.J., unpublished). However, the DA and DB axon guidance is only marginally affected in *unc-71* single mutants, and is not any worse in *unc-71; unc-6* double mutants than *unc-6* alone. Two main differences between the type D neurons and the DA and DB neurons, first noticed by Durbin (R. Durbin, PhD Thesis, University of Cambridge, 1987), may account for the differential effect of *unc-71*. First, the type D neurons extend their longitudinal axons immediately after the AVG neuron has extended its ventral process down the ventral midline, whereas the DA and DB motoneurons extend their longitudinal axons later. Second, the commissures of the type D neurons branch out of the longitudinal axons, whereas the commissures of the DA and DB neurons grow out directly from the cell bodies. Our study supports a model in which UNC-71 produced by the epidermis and neurons act as a short-range permissive cue to modulate

growth cone movement of specific classes of neurons in a temporally and spatially dynamic manner.

We thank J. McEwen for generation of *juIs76* and assistance in the screening of Max mutants; L. DeLong for additional mapping of *unc-71* and for obtaining YAC rescue; Y. Kohara for *unc-71* cDNAs; C. Bargmann for *kyIs136* marker; J. Kaplan for *glr-1* promoter and *nuIs25* marker; E. Lundquist for *unc-115* promoter; J. Harding for *jam-1* promoter; D. Pilgrim for *unc-119* promoter; M. Han for SUR-5::GFP and promoter; A. Fire for GFP vectors and the *myo-3* promoter; J. Plenefisch and E. Hedgecock for *pat-3(rh151)* allele; The *C. elegans* Genome Consortium for the sequences; S. Mitani for *tm347* and *tm353* and the knockout consortium for *ok265*; B. Podbilewicz for the use of unpublished observation; and the members of the Jin and Chisholm laboratories for suggestions on this work. Some of the strains used here were obtained from the Caenorhabditis Genetics Center, which is supported by the NIH. Y.J. is an assistant investigator of HHMI. This work was supported by NIH grant NS35546 to Y.J., GM50504 to M.J.S. and CA76713 to M.K.R.

REFERENCES

Altun-Gultekin, Z., Andachi, Y., Tsalik, L. T., Pilgrim, D., Kohara, Y. and Hobert, O. (2001). A regulatory cascade of three homeobox genes, *ceh-10*, *ttx-3* and *ceh-23*, controls cell fate specification of a defined interneuron class in *C. elegans*. *Development* **128**, 1951-1969.

Baum, P. D. and Garriga, G. (1997). Neuronal migrations and axon fasciculation are disrupted in ina-1 integrin mutants. *Neuron* **19**, 51-62.

Bigler, D., Chen, M., Waters, S. and White, J. M. (1997). A model for sperm-egg binding and fusion based on ADAMs and integrins. *Trends Cell Biol.* **7**, 220-225.

Black, R. A. and White, J. M. (1998). ADAMs: focus on the protease domain. *Curr. Opin. Cell Biol.* **10**, 654-659.

Blelloch, R. and Kimble, J. (1999). Control of organ shape by a secreted metalloprotease in the nematode *Caenorhabditis elegans*. *Nature* **399**, 586-590.

Brenner, S. (1974). The genetics of *Caenorhabditis elegans*. *Genetics* **77**, 71-94.

Burdine, R. D., Branda, C. S. and Stern, M. J. (1998). EGL-17 (FGF) expression coordinates the attraction of the migrating sex myoblasts with vulval induction in *C. elegans*. *Development* **125**, 1083-1093.

Chalfie, M., Tu, Y., Euskirchen, G., Ward, W. W. and Prasher, D. C. (1994). Green fluorescent protein as a marker for gene expression. *Science* **263**, 802-805.

Chen, E. B. and Stern, M. J. (1998). Understanding cell migration guidance: lessons from sex myoblast migration in *C. elegans*. *Trends Genet.* **14**, 322-327.

Chen, E. B., Branda, C. S. and Stern, M. J. (1997). Genetic enhancers of *sem-5* define components of the gonad-independent guidance mechanism controlling sex myoblast migration in *Caenorhabditis elegans* hermaphrodites. *Dev. Biol.* **182**, 88-100.

Cho, C., Ge, H., Branciforte, D., Primakoff, P. and Myles, D. G. (2000). Analysis of mouse fertilin in wild-type and fertilin $\beta^{-/-}$ sperm: evidence for C-terminal modification, α/β dimerization, and lack of essential role of fertilin α in sperm-egg fusion. *Dev. Biol.* **222**, 289-295.

Colavita, A. and Culotti, J. G. (1998). Suppressors of ectopic UNC-5 growth cone steering identify eight genes involved in axon guidance in *Caenorhabditis elegans*. *Dev. Biol.* **194**, 72-85.

Eto, K., Huet, C., Tarui, T., Kupriyanov, S., Liu, H. Z., Puzon-McLaughlin, W., Zhang, X. P., Sheppard, D., Engvall, E. and Takada, Y. (2002). Functional classification of ADAMs based on a conserved motif for binding to integrin $\alpha 9\beta 1$; implications for sperm-egg binding and other cell interactions. *J. Biol. Chem.* **277**, 17804-17810.

Evans, J. P. (2001). Fertilin β and other ADAMs as integrin ligands: insights into cell adhesion and fertilization. *BioEssays* **23**, 628-639.

Fambrough, D., Pan, D., Rubin, G. M. and Goodman, C. S. (1996). The cell surface metalloprotease/disintegrin Kuzbanian is required for axonal extension in Drosophila. *Proc. Natl. Acad. Sci. USA* **93**, 13233-13238.

Galko, M. J. and Tessier-Lavigne, M. (2000). Function of an axonal chemoattractant modulated by metalloprotease activity. *Science* **289**, 1365-1367.

George, S. E., Simokat, K., Hardin, J. and Chisholm, A. D. (1998). The VAB-1 Eph receptor tyrosine kinase functions in neural and epithelial morphogenesis in *C. elegans*. *Cell* **92**, 633-643.

Gettner, S. N., Kenyon, C. and Reichardt, L. F. (1995). Characterization of β *pat-3* heterodimers, a family of essential integrin receptors in C. elegans. *J. Cell Biol.* **129**, 1127-1141.

Gould, R. J., Polokoff, M. A., Friedman, P. A., Huang, T. F., Holt, J. C., Cook, J. J. and Niewiarowski, S. (1990). Disintegrins: a family of integrin inhibitory proteins from viper venoms. *Proc. Soc. Exp. Biol. Med.* **195**, 168-171.

Harfe, B. D., Vaz Gomes, A., Kenyon, C., Liu, J., Krause, M. and Fire, A. (1998). Analysis of a *Caenorhabditis elegans* Twist homolog identifies conserved and divergent aspects of mesodermal patterning. *Genes Dev.* **12**, 2623-2635.

Hart, A. C., Sims, S. and Kaplan, J. M. (1995). Synaptic code for sensory modalities revealed by *C. elegans* GLR-1 glutamate receptor. *Nature* **378**, 82-85.

Hattori, M., Osterfield, M. and Flanagan, J. G. (2000). Regulated cleavage of a contact-mediated axon repellent. *Science* **289**, 1360-1365.

Hedgecock, E. M., Culotti, J. G. and Hall, D. H. (1990). The *unc-5*, *unc-6* and *unc-40* genes guide circumferential migrations of pioneer axons and mesodermal cells on the epidermis in *C. elegans*. *Neuron* **4**, 61-85.

Huang, X., Cheng, H. J., Tessier-Lavigne, M. and Jin, Y. (2002). MAX-1, a novel PH/MyTH4/FERM domain cytoplasmic protein implicated in netrin-mediated axon repulsion. *Neuron* **34**, 563-576.

Hutter, H., Vogel, B. E., Plenefisch, J. D., Norris, C. R., Proenca, R. B., Spieth, J., Guo, C., Mastwal, S., Zhu, X., Scheel, J. et al. (2000). Conservation and novelty in the evolution of cell adhesion and extracellular matrix genes. *Science* **287**, 989-994.

Jin, Y., Hoskins, R. and Horvitz, H. R. (1994). Control of type-D GABAergic neuron differentiation by *C. elegans* UNC-30 homeodomain protein. *Nature* **372**, 780-783.

Jin, Y., Jorgensen, E., Hartwieg, E. and Horvitz, H. R. (1999). The *Caenorhabditis elegans* gene *unc-25* encodes glutamic acid decarboxylase and is required for synaptic transmission but not synaptic development. *J. Neurosci.* **19**, 539-548.

Koppen, M., Simske, J. S., Sims, P. A., Firestein, B. L., Hall, D. H., Radice, A. D., Rongo, C. and Hardin, J. D. (2001). Cooperative regulation of AJM-1 controls junctional integrity in *Caenorhabditis elegans* epithelia. *Nat. Cell Biol.* **3**, 983-991.

Lieber, T., Kidd, S. and Young, M. W. (2002). kuzbanian-mediated cleavage of Drosophila Notch. *Genes Dev.* **16**, 209-221.

Lundquist, E. A., Herman, R. K., Shaw, J. E. and Bargmann, C. I. (1998). UNC-115, a conserved protein with predicted LIM and actin-binding domains, mediates axon guidance in *C. elegans*. *Neuron* **21**, 385-392.

Maduro, M. and Pilgrim, D. (1995). Identification and cloning of *unc-119*, a gene expressed in the *Caenorhabditis elegans* nervous system. *Genetics* **141**, 977-988.

McIntire, S. L., Garriga, G., White, J., Jacobson, D. and Horvitz, H. R. (1992). Genes necessary for directed axonal elongation or fasciculation in *C. elegans*. *Neuron* **8**, 307-322.

Mello, C. C., Kramer, J. M., Stinchcomb, D. and Ambros, V. (1991). Efficient gene transfer in *C. elegans*: extrachromosomal maintenance and integration of transforming sequences. *EMBO J.* **10**, 3959-3970.

Miranti, C. K. and Brugge, J. S. (2002). Sensing the environment: a historical perspective on integrin signal transduction. *Nat. Cell Biol.* **4**, 83-90.

Nishiwaki, K., Hisamoto, N. and Matsumoto, K. (2000). A metalloprotease disintegrin that controls cell migration in *Caenorhabditis elegans*. *Science* **288**, 2205-2208.

Okkema, P. G., Harrison, S. W., Plunger, V., Aryana, A. and Fire, A. (1993). Sequence requirements for myosin gene expression and regulation in *Caenorhabditis elegans*. *Genetics* **135**, 385-404.

Pan, D. and Rubin, G. M. (1997). Kuzbanian controls proteolytic processing of Notch and mediates lateral inhibition during Drosophila and vertebrate neurogenesis. *Cell* **90**, 271-280.

Podbilewicz, B. (1996). ADM-1, a protein with metalloprotease- and disintegrin-like domains, is expressed in syncytial organs, sperm, and sheath cells of sensory organs in *Caenorhabditis elegans*. *Mol. Biol. Cell* **7**, 1877-1893.

Poinat, P., De Arcangelis, A., Sookhareea, S., Zhu, X., Hedgecock, E. M., Labouesse, M. and Georges-Labouesse, E. (2002). A conserved interaction between $\beta 1$ integrin/PAT-3 and Nck-interacting kinase/MIG-15

that mediates commissural axon navigation in *C. elegans*. *Curr. Biol.* **12**, 622-631.

Primakoff, P. and Myles, D. G. (2000). The ADAM gene family: surface proteins with adhesion and protease activity. *Trends Genet.* **16**, 83-87.

Qi, H., Rand, M. D., Wu, X., Sestan, N., Wang, W., Rakic, P., Xu, T. and Artavanis-Tsakonas, S. (1999). Processing of the notch ligand delta by the metalloprotease Kuzbanian. *Science* **283**, 91-94.

Rooke, J., Pan, D., Xu, T. and Rubin, G. M. (1996). KUZ, a conserved metalloprotease-disintegrin protein with two roles in Drosophila neurogenesis. *Science* **273**, 1227-1231.

Sambrook, J., Fritsch, E. F. and Maniatis, T. (1989). *Molecular Cloning: A Laboratory Manual*. Cold Spring Harbor, NY: Cold Spring Harbor Laboratory Press.

Schlondorff, J. and Blobel, C. P. (1999). Metalloprotease-disintegrins: modular proteins capable of promoting cell-cell interactions and triggering signals by protein-ectodomain shedding. *J. Cell Sci.* **112**, 3603-3617.

Seals, D. F. and Courtneidge, S. A. (2003). The ADAMs family of the metalloprotease: multidomain proteins with multiple functions. *Genes Dev.* **17**, 7-30.

Siddiqui, S. S. (1990). Mutation affecting axonal growth and guidance of motor neurons and mechanosensory neurons in the nematode *Caenorhabditis elegans*. *Neurosci. Res. Suppl. 13*, S171-S190.

Siddiqui, S. S. and Culotti, J. G. (1991). Examination of neurons in wild type and mutants of *Caenorhabditis elegans* using antibodies to horseradish peroxidase. *J. Neurogenet.* **7**, 193-211.

Stein, L., Sternberg, P., Durbin, R., Thierry-Mieg, J. and Spieth, J. (2001). WormBase: network access to the genome and biology of *Caenorhabditis elegans*. *Nucleic Acids Res.* **29**, 82-86.

Steven, R., Kubiseski, T. J., Zheng, H., Kulkarni, S., Mancillas, J., Ruiz Morales, A., Hogue, C. W., Pawson, T. and Culotti, J. (1998). UNC-73 activates the Rac GTPase and is required for cell and growth cone migration in *C. elegans*. *Cell* **92**, 785-795.

Stringham, E., Pujol, N., Vanderkerckhove, J. and Bogaert, T. (2002). *unc-53* controls longitudinal migration in *C. elegans*. *Development* **129**, 3367-3379.

Sulston, J. E. and Horvitz, H. R. (1977). Post-embryonic cell lineages of the nematode, *Caenorhabditis elegans*. *Dev. Biol.* **56**, 110-156.

Sulston, J. E., Schierenberg, E., White, J. G. and Thomson, J. N. (1983). The embryonic cell lineage of the nematode *Caenorhabditis elegans*. *Dev. Biol.* **100**, 64-119.

Tessier-Lavigne, M. and Goodman, C. S. (1996). The molecular biology of axon guidance. *Science* **274**, 1123-1133.

The *C. elegans* Genome Consortium (1998). Genome sequence of the nematode *C. elegans*: a platform for investigating biology. *Science* **282**, 2012-2018.

Thomas, J. H., Stern, M. J. and Horvitz, H. R. (1990). Cell interactions coordinate the development of the *C. elegans* egg-laying system. *Cell* **62**, 1041-1052.

Van Eerdewegh, P., Little, R. D., Dupuis, J., Del Mastro, R. G., Falls, K., Simon, J., Torrey, D., Pandit, S., Mckenny, J., Braunschweiger, K. et al., (2002). Association of the ADAM33 gene with asthma and bronchial hyperresponsiveness. *Nature* **418**, 426-430.

Wadsworth, W. G., Bhatt, H. and Hedgecock, E. M. (1996). Neuroglia and pioneer neurons express UNC-6 to provide global and local netrin cues for guiding migrations in *C. elegans*. *Neuron* **16**, 35-46.

Wadsworth, W. G. (2002). Moving around in a worm: netrin UNC-6 and circumferential axon guidance in *C. elegans*. *Trends Neurosci.* **25**, 423-429.

Waters, S. I. and White, J. M. (1997). Biochemical and molecular characterization of bovine fertilin α and β (ADAM 1 and ADAM 2): a candidate sperm-egg binding/fusion complex. *Biol. Reprod.* **56**, 1245-1254.

Wen, C., Metzstein, M. M. and Greenwald, I. (1997). SUP-17, a *Caenorhabditis elegans* ADAM protein related to Drosophila KUZBANIAN, and its role in LIN-12/NOTCH signalling. *Development* **124**, 4759-4767.

White, J. G., Southgate, E., Thomson, J. N. and Brenner, S. (1986). The structure of the nervous system of the nematode *Caenorhabditis elegans*. *Philos. Trans. R. Soc. Lond. B* **314**, 1-340.

Wicks, S. R., Yeh, R. T., Gish, W. R., Waterston, R. H. and Plasterk, R. H. (2001). Rapid gene mapping in *Caenorhabditis elegans* using a high density polymorphism map. *Nat. Genet.* **28**, 160-164.

Williams, B. D. and Waterston, R. H. (1994). Genes critical for muscle development and function in *Caenorhabditis elegans* identified through lethal mutations. *J. Cell Biol.* **124**, 475-490.

Wolfsberg, T. G., Primakoff, P., Myles, D. G. and White, J. M. (1995). ADAM, a novel family of membrane proteins containing a disintegrin and metalloprotease domain: multipotential functions in cell-cell and cell-matrix interactions. *J. Cell Biol.* **131**, 275-278.

Yochem, J., Gu, T. and Han, M. (1998). A new marker for mosaic analysis in *Caenorhabditis elegans* indicates a fusion between hyp6 and hyp7, two major components of the hypodermis. *Genetics* **149**, 1323-1334.

Zhu, X., Bansal, N. P. and Evans, J. P. (2000). Identification of key functional amino acids of the mouse fertilin β (ADAM2) disintegrin loop for cell-cell adhesion during fertilization. *J. Biol. Chem.* **275**, 7677-7683.